Abstract No: A-169

QUANTIFYING ABOVE AND BELOWGROUND CARBON LOSS FOLLOWING WILDFIRE IN PEATLANDS USING REPEATED LIDAR MEASUREMENTS

Todd J. Hawbaker[1*], Ashwan D. Reddy[2], Zhiliang Zhu[3], Fredric C. Wurster[4], and Jamie A. Duberstein[5]

[1]U.S. Geological Survey, Denver, CO, USA;
[2]University of Maryland, College Park, MD, USA;
[3]U.S. Geological Survey, Reston, VA, USA;
[4]U.S. Fish and Wildlife Service, Suffolk, VA, USA;
[5]Clemson University, Clemson, SC, USA

**Corresponding author: tjhawbaker@usgs.gov*

SUMMARY

Natural disturbances like fires are often unavoidable and their negative effects in peatlands can be amplified by concomitant human-driven changes such as artificial drainage. This study used pre- and post-fire airborne lidar to estimate aboveground and belowground carbon loss as a result of the South One and Lateral West Fires which burned 24 and 25 km^2 in 2008 and 2011, respectively in the Great Dismal Swamp National Wildlife Refuge, Virginia and North Carolina, USA. Total carbon lost from the 2 fires was 0.60 and 1.23 Tg C, respectively. Our results demonstrate the value of sustained lidar data collection efforts to quantify the impacts of ecosystem disturbances on carbon cycling. Our findings document that fires in drained peatlands can result in substantial amounts of belowground carbon loss that could potentially be avoided by restoring drained and protecting existing peatlands.

Keywords: *lidar, fire, carbon, biomass consumption*

INTRODUCTION

Globally, peatlands hold between 16 and 33% of global soil carbon stocks even though they account for just 3% of the land surface (Bridgham *et al.,* 2006). Peatlands can contribute methane (CH_4) to the atmosphere as a result of methanogenesis in the anaerobic conditions present in saturated soils. Over extended time periods, however, peatlands sequester carbon from the atmosphere and develop large belowground carbon (C) stocks as vegetation falls to the ground and decomposes at relatively slow rates that are influenced by soil saturation and litter quality (Bridgham *et al.,* 2006; Day, 1982). Because their potential to sequester carbon from the atmosphere is offset by CH_4 emissions, peatlands are valued for the large C stocks they hold and not necessarily their sequestration rates (Bridgham *et al.,* 2006); preventing the loss of those C stocks is a pressing concern for agencies managing peatlands.

Human-driven changes in land use and management are a primary threat to the C stored in peatlands. These changes include drainage through canal construction, forest harvest, peat harvesting, and conversion to agriculture. Threats to peatlands are especially evident in the southeastern United States where legacies of land use have altered the hydrology, disturbance regimes, and vegetation dynamics of peatlands, and made vulnerable the large stocks of C stored within them (Batzer and Baldwin, 2012). Specifically, past efforts to drain peatlands have altered the hydrology and disrupted historic carbon cycling patterns. The effects of these changes on C include direct oxidation of peat, decreased peat accretion rates, and increased severity of fires resulting in loss of both above and belowground biomass. Consequently, peatlands in the southeastern U.S. are the focus of many management efforts to mitigate and reduce the negative impacts of past land use.

Consistent monitoring of C stocks and changes in C stocks is essential to understanding how land management and natural disturbances influence the ability of peatlands and other ecosystems to sequester carbon dioxide from the atmosphere and offset anthropogenic greenhouse gas emissions. Light-detection and ranging (lidar) is one technology that can be utilized to monitor changes in above and belowground C stocks because of its ability to characterize surface elevations and vegetation heights. In contrast to traditional field surveys, lidar can provide continuous coverage over large areas (Lefsky *et al.,* 2002; Ballhorn *et al.,* 2009). However, challenges remain in quantifying change with lidar data because there is no concerted effort to repeatedly collect lidar in the U.S. and most data collection efforts are designed for constructing digital elevation models with pulse densities lower than ideal for monitoring vegetation. The lidar data that do exist were collected under varying vegetation conditions and have differences in pulse densities and pulse footprints of the lidar collections. Most lidar-based

biomass mapping efforts have relied on relating forest inventory data to lidar collected during coincident time periods; methods to relate forest inventory data collected at one time period to lidar collections from multiple time periods have not been as well developed, but would be valuable to facilitate consistent, cost-effective monitoring of biomass, C stocks, and disturbances.

To better understand how disturbances affect carbon stocks in peatlands and identify ways to overcome the challenges of using repeated lidar measurements, we conducted this study with two goals: (1) to determine how well repeated lidar measurements can be used to monitor changes in above and belowground C stocks in forested peatlands in the southeastern U.S., and (2) to estimate the amount of aboveground and belowground C lost following two recent fires in the Great Dismal Swamp.

METHODS

Study Area

Our study was conducted within the 450 km^2 Great Dismal Swamp National Wildlife Refuge and Dismal Swamp State Natural Area located in the southeastern U.S. (referred to as Great Dismal Swamp or GDS). Prior to becoming a refuge, the land was owned by several timber companies that built a 158-mile network of roads and canals to drain the wetland and facilitate timber harvesting. Most of the canals in the GDS were constructed between 1954 and 1968 (USGS, 1954, 1968) and are thought to have created drier conditions throughout the swamp, contributing to peat subsidence, decreased C stocks and sequestration rates, changes in vegetation communities, and increased fire severity (USFWS, 2006).

Present-day vegetation in GDS is dominated by several forest types, often with very dense shrub understories. These forest types include (1) bald cypress (*Taxodium distichum*)/black gum (*Nyssa sylvatica*) mix, (2) Atlantic white cedar (*Chamaecyparis thyoides*), (3) red maple (*Acer rubrum*)/blackgum mix, and (4) tall pond pine (*Pinus serotina*) pocosins. The type of forest present at any location is a result of disturbance and management and hydrologic conditions, especially duration of soil saturation (Dabel and Day, 1977; Carter *et al.*, 1994).

On August 4, 2011, lightning ignited the 'Lateral West' fire within the refuge that burned 25 km^2 over 126 days. That fire overlapped with the areas burned in the 2008 'South One' fire (24 km^2) and the 2006 'West Drummond' fire (2.3 km^2). Few trees were left standing in areas affected by these three fires and soil loss of more than 1 meter was observed in some areas.

Field Data Collection and Analysis

To estimate aboveground biomass, tree data were collected at 76 plots located in unburned areas throughout the GDS during the summer of 2014. At each location, we established a 5.6 m fixed-radius plot (100 m^2) and recorded the species, status (*e.g.*, live or dead), and measured the diameter of all trees with diameter at breast height ≥ 2.54 cm. For a subset of trees, selected using a prism with a basal area factor of 2 m^2/ha, we also measured total tree height using a Haglöf Vertex Laser Hypsometer. Biomass of each tree was calculated using allometric equations (Jenkins et al., 2003), and summed to generate plot-level totals of live tree aboveground biomass (referred to as biomass from here on). The location of each plot was recorded with a Trimble ProXH global positioning system (GPS) and post-processed to differentially correct the locations. Horizontal accuracy of the post-processed GPS locations ranged between 0.1 and 0.9 m and averaged 0.4 m.

Soil bulk density and carbon content analysis were calculated for 23 samples collected at unburned locations in areas near the Lateral West fire in August 2013 and 3 samples from a previous 1999 study (NRCS Soil Survey Lab in Lincoln, NE, USA). Bulk density ranged from 0.09 to 0.24 g/cm^3 and had a mean of 0.16 g/cm^3. Carbon content was between 46 and 64% of total soil matter, with a mean of 59%. Consistent with the characteristics of peatland soils, organic matter averaged 95% among all samples. Mean values for bulk density and carbon content were used to convert elevation change to carbon loss.

Lidar Data Collection and Analysis

Lidar flights were made in 2006, 2010, 2012, and 2014, parts of which were overlapping. These collections were made with similar flight and sensor characteristics, but during different times of year (Table 1). We selected lidar pulse returns within 5.6 m radius of our 2014 field plot centers from each collection. We derived the surface elevations and canopy height data from each lidar collection to build a series of regression models at the plot level for predicting biomass at the landscape level. To generate landscape-level results, all lidar pulses were assigned to 10 x 10 m grid cells, to match the area of the field plots (100 m_2).

Table 1. Characteristics of lidar collections overlapping the Great Dismal Swamp.

Collection	Year	Month	Pulse density (#/m^2)
Chesapeake County	2006	Sep.	1 pulse / m2
Great Dismal Swamp (GDS)	2010	Mar.	2 pulses / m2
Lateral West Burned Area	2012	Aug.	2 pulses / m2
North Carolina	2014	Mar. & Apr.	4 pulses / m2

We estimated plot-level elevation for each lidar collection using the mean of the lowest three elevation values per plot or grid-cell. When compared to the 2010 GDS-wide elevation models, the 2006 elevation model had significantly higher surface elevations in vegetated areas (0.62 m difference; t-test p-value=0.0002). This was likely a result of the lower pulse density in the 2006 data. Therefore, we related 2010 and 2006 elevations to each other using a simple linear regression, and then applied the regression to adjust the 2006 elevations (intercept=1.0; slope=0.72; R^2=0.71; RMSE=0.41). A second t-test of the adjusted 2006 elevations confirmed that they were not significantly different from the 2010 elevations (0.02 m difference; p-value=0.86). T-tests comparing the 2012 and 2014 elevations to the 2010 elevations were not significant (difference=0.02 m; p-value=0.93 for 2012 vs. 2010; difference=0.16 m; p-value=0.14 for 2014 vs. 2010). The differences in elevation models across collections were minimal, especially after adjusting the 2006 data, providing confidence that lidar-derived vegetation heights would be consistent across the collections.

Potential predictor variables for biomass were generated for both the plot-level and landscape-level data by calculating the mean and standard deviation of lidar pulse heights, and mean of the highest five pulses heights. We fit a series of regressions using the individual predictors and all combinations of two predictors to determine which of the 2014 lidar canopy metrics were most strongly related to biomass measured in 2014 at the plot locations. All variables were natural-log + 1 transformed prior to analysis. The fit regressions were used to predict biomass for all plots and all lidar collections. We calculated the average of plot-level standard deviation in biomass over time as an instability metric to further evaluate the models; larger values indicate that the predictions are less consistent (i.e. less stable) across the different lidar collections. We selected the most stable regression to make landscape-level predictions of biomass for the four different lidar collections.

To scale up our results to the entire GDS, we applied the methods used for the plot-level lidar analysis to each lidar collection, calculating and adjusting elevation and vegetation heights, and predicting biomass within 10 x 10 m^2 grid cells. Changes in surface elevations and belowground C stocks within the South One and Lateral West fire perimeters were estimated by differencing elevation data from either the 2010 and 2006 or 2012 and 2010 lidar collections, calculating total volume of change, and then multiplying that volume by bulk density and carbon content values, following methods outlined in Reddy *et al.* (2014). Elevation change and belowground C loss were calculated for the portion of the South One fire that was also covered by the 2006 lidar collection. Similarly, changes in biomass within the South One and Lateral West fire perimeters were estimated by differencing biomass data from either the 2010 and 2006 or 2012 and 2010 collections (depending on the fire) and then multiplying the biomass values by 0.5 to convert to C (Jenkins *et al.*, 2003).

RESULTS

Of the six models fit for this study, significant relationships (slope coefficient p-values < 0.05) between biomass and the predictors were only identified for the univariate models. Error rates and R^2 values were similar across the three univariate models (Table 2). The regression predicting biomass using the mean of the highest five pulse returns (H.max) had the greatest stability in biomass predictions (instability = 6.5 kg/m^2); all other models had greater instability measures (7.3 or larger). Thus, landscape-level predictions of biomass were made with the regression using mean of the highest five pulse heights (H.max) as a predictor.

Table 2. Regressions of live tree aboveground biomass vs. lidar height summaries; H.max = mean of highest five lidar pulses; H.mean = mean of lidar pulse heights; H.sd = standard deviation of lidar pulse heights; ln = natural log. Significant level of regression coefficients: ' 0.1; * 0.05; ** 0.01; *** 0.001.

Model form	RMSE	R^2	Instability
ln(biomass+1) = -4.41* + 2.31 × ln(H.max+1)***	0.65	0.30	6.48
ln(biomass+1) = -2.24* + 1.96 × ln(H.mean+1)***	0.63	0.33	8.73
ln(biomass+1) = -0.53 + 1.82 × ln(H.sd+1)***	0.64	0.31	7.34
ln(biomass+1) = -2.43 + 1.04 × ln(H.max+1) + 1.08 × ln(H.sd+1)	0.65	0.30	7.10
ln(biomass+1) = -1.97' + 1.22 × ln(H.mean+1)' + 0.89 × ln(H.sd+1)	0.63	0.34	8.15
ln(biomass+1) = -3.77* + 1.28 × ln(H.max+1)' + 1.05 × ln(H.sd+1)	0.63	0.34	8.30

For the South One fire, average elevation decrease was 0.17 m and belowground C loss was 16.0 kg/m^2 (Figure 1). With these C loss rates, total belowground C loss from the entire South One fire was 0.38 Tg C. There

is a large degree of uncertainty around this estimate as there are visible patterns in the 2006 to 2010 elevation change maps outside the fire perimeter that are likely artifacts of the different lidar collections and not true elevation change. The Lateral West fire occurred 3 years after the South One fire and burned almost the exact same area, resulting in an additional decrease in elevation of 0.46 m (mean within the perimeter). This resulted in a loss of 43.4 kg C/m^2 or a total of 1.09 Tg C. These estimates are nearly identical to those made in our previous study using slightly different methods (Reddy *et al.*, 2014).

Patterns of aboveground biomass change were more pronounced than elevation change in both the South One and Lateral West perimeters (Figure 2). Average aboveground C loss within the portion of the South One perimeter covered by the 2006 lidar collection was 4.5 kg C/m^2, resulting in a total loss of 0.13 Tg C. Within the entire South One perimeter, total aboveground C loss was 0.22 Tg C. Aboveground C lost in the Lateral West fire was less than in the South One fire, averaging 2.8 kg C/m^2 and totaling 0.14 Tg C.

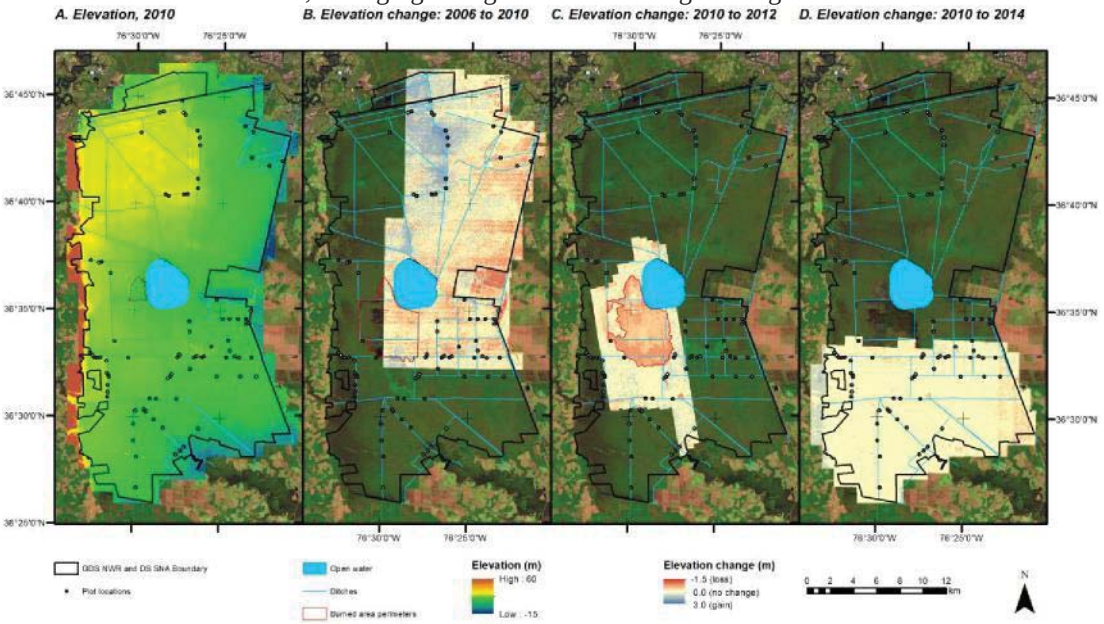

Figure 1. Lidar-derived elevation for 2010 (A), and elevation change between 2006 and 2010 (B), 2010 and 2012 (C), and 2010 and 2014 (D) for the Great Dismal Swamp National Wildlife Refuge (GDS NWR) and Dismal Swamp State Natural Area (DS SNA). The area over which changes were calculated was limited by the extent of the 2006, 2012, and 2014 lidar collections. Landsat 8 bands 7-4-2 from Feb. 28, 2014, in background.

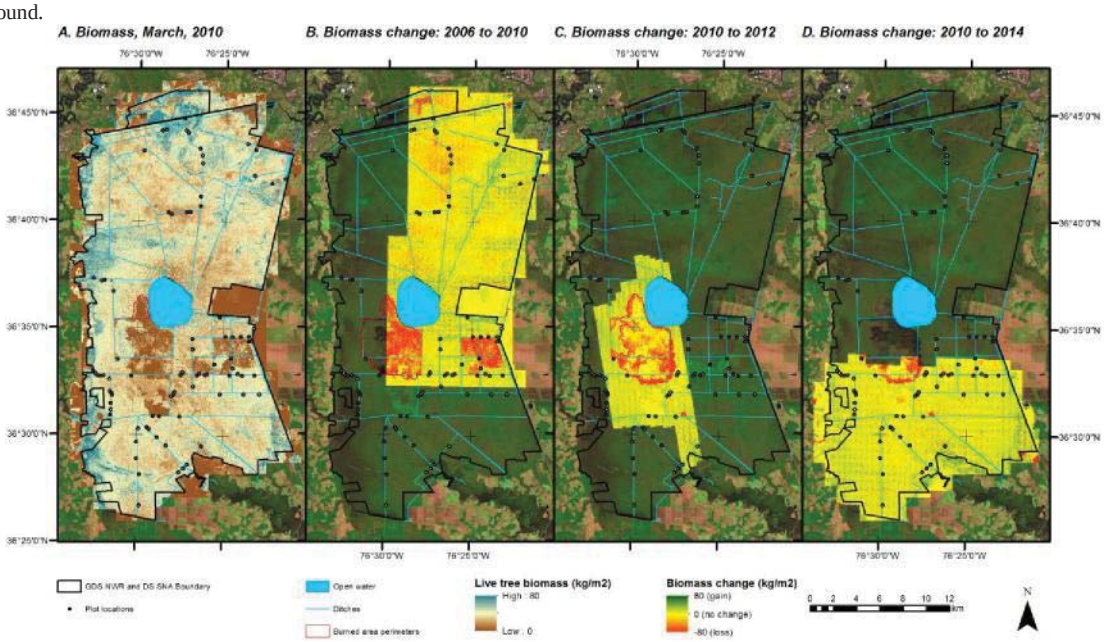

Figure 2. Lidar-derived biomass for 2010 (A), and biomass change between 2006 and 2010 (B), 2010 and 2012 (C), and 2010 and 2014 (D) for the Great Dismal Swamp National Wildlife Refuge (GDS NWR) and Dismal Swamp State Natural Area (DS SNA). Landsat 8 bands 7- 4-2 from Feb. 28, 2014, in background. The area over which changes were calculated was limited by the extent of the 2006, 2012, and 2014 lidar collections.

DISCUSSION

Between 2008 and 2011, two large fires burned 5.6% of the area of the Great Dismal Swamp. Using repeated lidar height measurements, we assessed the impacts of those fires on above and belowground C. The South One fire in 2008 consumed a total of 0.60 Tg C and 63% of that was belowground. The loss of canopy cover and exposure of previously buried peat deposits after the South One fire created conditions that amplified the severity of the later Lateral West fire in 2011, which consumed 1.23 Tg C, 88% of which was belowground. An accurate peat-depth map does not exist for the GDS so it was not possible to estimate total belowground C stocks in the GDS and the proportion that was lost in the two fires. However, the impacts of the fires on belowground C will be long lasting. Average peat accumulation rates are 0.07 cm/year in the conterminous U.S. (Bridgham *et al.,* 2006), and at this rate, recovery of peat in the burned areas would take nearly 900 years.

A complete aboveground biomass dataset for the GDS was based on the 2010 lidar flight data (Figure 2). Total biomass in the GDS in 2010 after the 2006 South One fire and other disturbances (e.g. harvest shown in Figure 2) was 4.50 Tg C. The 2011 Lateral West fire consumed 3% of that. Normally, we would expect aboveground biomass to recover over a period of several decades. However, following the fire, much of the burned area filled with water, creating a lake, which will impede revegetation of this area. Given that the burned area now holds standing water, it is difficult to predict when the aboveground C lost in the South One and Lateral West fires will be recovered.

Fire is a natural and historically frequently occurring process that plays an important role driving vegetation succession in the forest types present in the GDS (Frost, 1993). Extensive drainage of the GDS through canal construction has altered hydrologic conditions, leaving GDS much drier than it was historically. Consequently, fires substantially change C storage and in some cases result in a state change from forested swamps to open water. These changes could potentially be mitigated by managing the hydrology of GDS for wetter soil conditions so that when fires do occur, primarily aboveground C stocks are consumed and belowground C stocks are left intact.

CONCLUSION

Making use of repeated lidar collections for monitoring forest biomass has been challenging because of differences in flight and sensor configurations and vegetation conditions. The methods used in this study demonstrate an approach that may be promising to overcome those challenges. Using an approach along these lines may help to extend the amount of lidar information that is usable to monitor changes in forest vegetation and biomass when temporally coincident forest inventories are not available.

REFERENCES

1. Ballhorn U., F. Siegert, M. Mason, S. Limin. 2009. Derivation of burn scar depths and estimation of carbon emissions with LIDAR in Indonesian peatlands. Proceedings of the National Academy of Sciences, 106:21213-21218
2. Batzer, D.P. and A.H. Baldwin (editors). 2012. Wetland Habitats of North America; Ecology and Conservation Concerns. University of California Press, Berkeley, CA, USA, 389 p.
3. Bridgham, S.D., J.P. Megonigal, J.K. Keller, N.B. Bliss, and C. Trettin. 2006. The Carbon Balance of North American Wetlands. Wetlands, 26:889-916
4. Dabel, C.V. and F.P. Day. 1977. Structural comparisons of four plant communities in the Great Dismal Swamp, Virginia. Bulletin of the Torrey Botanical Club, 104:352-360
5. Day, F.P. 1982. Litter decomposition rates in the seasonally flooded Great Dismal Swamp. Ecology, 63:670-678 Carter, V., P.T. Gammon and M.K. Garrett. 1994. Ecotone dynamics and boundary determination in the Great Dismal Swamp. Ecological Applications, 4:189–203
6. Frost, C.C. Presettlement fire regimes in southeastern marshes, peatlands, and swamps. Pages 39-60 in Proceedings of the 19th Tall Timbers Fire Ecology Conference, Nov. 3-6, 1993, Tallahassee, FL
7. Jenkins, J.C., D.C. Chojnacky, L.S. Heath, and R.A. Birdsey. 2003. National-scale biomass estimators for United States tree species. Forest Science, 49:12-35
8. Lefsky, M.A., W.B. Cohen, D.J. Harding, G.G. Parker, S.A. Ackerand S.T. Gower. 2002. LiDAR remote sensing of aboveground biomass in three biomes. Global Ecology and Biogeography, 11:393–399
9. Reddy, A.D., T.J. Hawbaker, F. Wurster, Z. Zhu, S. Ward, D. Newcomb, and R. Murray. 2015. Quantifying soil carbon loss and uncertainty from a peatland wildfire using multi-temporal lidar, Remote Sensing of Environment 170:306-316
10. U.S. Fish and Wildlife Service (USFWS). 2006. *Great Dismal Swamp National Wildlife Refuge and Nansemond National Wildlife Refuge Final Comprehensive Conservation Plan*. 258 p.
11. U.S. Geological Survey (USGS). 1954. Topographic maps (*variously named*) 1:7,500, 1 sheet each.
12. U.S. Geological Survey (USGS). 1968. Topographic maps (*variously named*) 1:7,500, 1 sheet each